IMPLICATIONS OF THE INTER-PERIOD CORRELATION OF STRONG GROUND MOTIONS ON STRUCTURAL RISK

J Bayless[1] and NA Abrahamson[2]

ABSTRACT

In this paper, we demonstrate that the inter-period correlation of epsilon (ρ_ϵ) is an essential component of ground motion simulation validation when the simulations are used in fragility or risk applications. To perform this demonstration, we generate large suites of scenario ground motion simulations using the point source stochastic method. Two compatible suites of simulations are developed for the selected ground motion levels; one suite without any imposed inter-period correlation, and one with FAS ϵ sampled from a multivariate normal distribution with covariance specified by our empirical model for ρ_ϵ of FAS. Both suites of simulations are inverse transformed to the time domain and applied in dynamic nonlinear structural analyses, using the open source finite-element platform, OpenSees. We evaluate the response using nonlinear structural models, and develop structural fragility curves. Finally, we illustrate how the effect of ρ_ϵ propagates through to seismic risk calculations by combining the fragility curves with generic seismic hazard curves for California. The character of ρ_ϵ is found to have a meaningful impact on structural response variability, and therefore seismic risk. The suite of simulations with the imposed ρ_ϵ leads to a larger variability in structural response, flatter structural fragility curves, and higher seismic risk, compared with the simulations generated without the appropriate ρ_ϵ. This conclusion reinforces the importance of validating ρ_ϵ in ground motion simulations prior to their use in fragility or risk applications.

[1]Graduate Student Researcher, Dept. of Civil Eng., University of California, Davis, 95616 (jrbayless@ucdavis.edu)
[2]Chief Seismologist, Pacific Gas & Electric, San Francisco, CA 94105

Implications of the inter-period correlation of strong ground motions on structural risk

J Bayless[1] and NA Abrahamson[2]

ABSTRACT

In this paper, we demonstrate that the inter-period correlation of epsilon ($\boldsymbol{\rho_\epsilon}$) is an essential component of ground motion simulation validation, particularly when the simulations are used in structural fragility or risk applications. To perform this demonstration, we generate large suites of scenario ground motion simulations using the point source stochastic method. Two compatible suites of simulations are developed for each selected ground motion level; one suite without any imposed inter-period correlation, and a second with Fourier amplitude spectra (FAS) epsilon sampled from a multivariate normal distribution with covariance specified by our empirical model for $\boldsymbol{\rho_\epsilon}$ of FAS. Both suites of simulations are inverse transformed to the time domain and applied in dynamic nonlinear structural analyses, using the open source finite-element platform, OpenSees. We evaluate the response using nonlinear structural models, and develop structural fragility curves. Finally, we illustrate how the effect of $\boldsymbol{\rho_\epsilon}$ propagates through to seismic risk calculations by combining the fragility curves with generic seismic hazard curves for California. The character of $\boldsymbol{\rho_\epsilon}$ is found to have a meaningful impact on structural response variability, and therefore seismic risk. The suite of simulations with the imposed $\boldsymbol{\rho_\epsilon}$ leads to a larger variability in structural response, flatter structural fragility curves, and higher seismic risk, compared with the simulations generated without the appropriate $\boldsymbol{\rho_\epsilon}$. This conclusion reinforces the importance of validating $\boldsymbol{\rho_\epsilon}$ in ground motion simulations prior to their use in fragility or risk applications.

1. Introduction

Residuals from empirical ground-motion models (GMMs, also known as ground-motion prediction equations, GMPEs) are typically partitioned into between-event residual (δB), and within-event residuals (δW), following the notation of Al Atik et al., (2010). The between-event residual is the average difference between the observed IM from a specific earthquake and the median spectral acceleration predicted by the GMM. The within-event residual (δW) is the difference between the spectral acceleration at a specific site for a given earthquake and the median spectral acceleration predicted by the GMM plus δB. The residual components δB and δW are zero-mean, independent, normally distributed random variables with standard deviations τ and ϕ, respectively [1]. GMM residuals are converted to epsilon (ϵ) by normalizing the residuals by their standard deviation. Epsilon of between-event residuals (ϵ_B) and epsilon of within-event residuals (ϵ_W) are the individual residual components normalized by their respective standard deviations. Because of the normalization, the random variables ϵ_B and ϵ_W are well represented by a standard-

[1]Graduate Student Researcher, Dept. of Civil Eng., University of California, Davis, 95616 (jrbayless@ucdavis.edu)
[2]Chief Seismologist, Pacific Gas & Electric, San Francisco, CA 94105

normal distribution (mean=0, variance=1). If the total residual is used, then the resulting ϵ_{total} will, in general, not have zero mean due to the uneven sampling of earthquakes in the data set. In this paper, we work with epsilon of the within-event residuals, because the within-event residual standard deviation controls the total correlation and they have zero mean. For notational brevity, the 'W' subscript is dropped and the term ϵ refers to within-event epsilon herein.

The values of ϵ at neighboring periods (T) are generally correlated. For example, if a ground motion is stronger than average at $T=1.0$ s, then it is likely to also be stronger than expected at adjacent periods, e.g. $T=0.8$ s or $T=1.2$ s. However, for a widely-spaced period pair (e.g. $T=10.0$ s compared with $T=1.0$ s) one might expect that the relative magnitude of the within-event residual at $T=10.0$ s behaves independently of the $T=1.0$ s ordinate. The inter-period correlation of ϵ quantifies this probabilistic relationship of ϵ values between periods.

The correlation coefficient of two random variables is a measure of their linear dependence. In this case, ϵ calculated from a large set of ground motions at different frequencies (f) are random variables. The correlation coefficient between $\epsilon(f_1)$ and $\epsilon(f_2)$ can be estimated using a maximum likelihood estimator, the Pearson-product-moment correlation coefficient, ρ [2]. The correlation coefficient for a sample of ϵ at frequencies f_1 and f_2 is given by Eq. 1:

$$\rho_{\epsilon(f_1),\epsilon(f_2)} = \frac{cov\big(\epsilon(f_1),\epsilon(f_2)\big)}{\sigma_{\epsilon(f_1)}\sigma_{\epsilon(f_2)}} = \frac{\sum_{i=1}^{n}\big(\epsilon_i(f_1)-\overline{\epsilon(f_1)}\big)\big(\epsilon_i(f_2)-\overline{\epsilon(f_2)}\big)}{\sqrt{\sum_{i=1}^{n}\big(\epsilon_i(f_1)-\overline{\epsilon(f_1)}\big)^2}\sqrt{\sum_{i=1}^{n}\big(\epsilon_i(f_2)-\overline{\epsilon(f_2)}\big)^2}} \tag{1}$$

where cov is the covariance, σ is the standard deviation, n is the total number of observations, i is the ith observation of ϵ, and $\overline{\epsilon(f_1)}$ and $\overline{\epsilon(f_2)}$ are the sample means of ϵ at frequencies f_1 and f_2, respectively. In our applications, $\bar{\epsilon}$ is equal to zero because we use within-event residuals, indicating that the GMM is centered. The relation for $\rho_{\epsilon(f_1),\epsilon(f_2)}$ given in Eq. 1 is reciprocal; the correlation coefficient between two given frequencies is the same regardless of which frequency is the conditioning frequency.

Using a database of within-event residuals, the calculation of $\rho_{\epsilon(f_1),\epsilon(f_2)}$ can be repeated for every frequency pair of interest. Fig. 1 shows a graphical representation of this step at three example frequency pairs. The resulting correlation coefficients for each pair of frequencies can be saved as tables (e.g. [3], [4], [5], [6], [7]), or can be empirically modeled. For modern GMMs, models of the correlation of ϵ are commonly created for PSA (e.g. [8], [9], [10], [11], [12], [3]). Recently, correlation models for ϵ from Fourier amplitude spectra (FAS) have also been developed (e.g. [13], [14]).
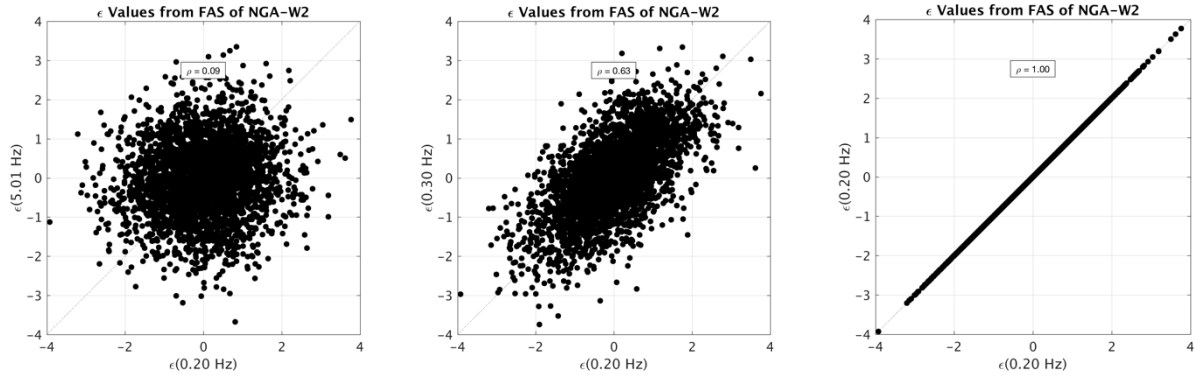
Figure 1. ϵ values at pairs of frequencies calculated from a database of ground motions, exhibiting the correlation dependent on frequency spacing. Left: $f_1 = 0.2$ Hz and $f_2 = 5.0$ Hz. Middle: $f_1 = 0.2$ Hz and $f_2 = 0.3$ Hz. Right: $f_1 = 0.2$ Hz and $f_2 = 0.2$ Hz

Physical Meaning and Relevance of ρ_ϵ

The physical meaning of ρ_ϵ may not be commonly known to earthquake engineers. The parameter ϵ itself is an indicator of the peaks and troughs at a given frequency in a spectrum. Since ρ_ϵ is a measure of the linear dependence of ϵ between two frequencies, ρ_ϵ characterizes the relative width of these extrema. For example, very high ρ_ϵ (values close to one) over broad frequency pairs indicate wide peaks and troughs in the spectra; leading to smoother undulating spectra. Conversely, very low ρ_ϵ (values close to zero) between neighboring frequency pairs indicate very narrow peaks and troughs; leading to 'noisy' looking spectra.

The generic term 'spectra' can refer to either PSA or FAS. PSA spectra are the peak response from a single degree of freedom oscillator system. PSA spectra are influenced by a range of frequencies, and the breadth of that range is dependent on the oscillator period [14]. The FAS provides a more direct representation of the frequency content of the ground motions, and since the Fourier transform is a linear operation, the FAS is a much more straightforward representation of the ground motion. This simpler behavior makes the FAS preferable over PSA for incorporating inter-period correlation into numerical methods for ground-motion simulations, and this is the IM we adopt.

Since ρ_ϵ is a measure of the width of spectral peaks, it has relevance in dynamic structural response. For linear response, a structure will be sensitive to the frequency content over a range of frequencies about the natural frequency of the structures. For the uncorrelated case, if the ϵ value at the natural frequencies is a high positive value (corresponding to a peak), the values of ϵ at the nearby frequencies will be randomly high or low so the response of the structure will increase a small factor; however, for the correlated case, the values of ϵ at the nearby frequencies will tend to also be positive values so the response of the structure will increase a larger factor. During nonlinear seismic response, the effect of the correlation can be even greater than for linear response. For nonlinear response, structures can experience softening characterized by elongation of their natural vibration period ([15], [16]). This occurs when damage to the structural elements leads to large strains which reduce the effective stiffness and effective damping. As a structure softens and its effective fundamental period (a first order indicator of seismic damage) increases

and the response will depend on if the structure is softening into a peak or a trough in the frequency content. For the correlated case, the chance of softening into a peak or a trough will depend on the breadth of a ground motion spectral peak or trough, thereby affecting the structural response. The aggregate effect is the variability in structural response is higher for ground motions with realistic ρ_ϵ than for ground motions with unrealistically low ρ_ϵ, as we demonstrate in the following sections of this paper.

Paper Organization

In this paper, we demonstrate that the characteristics of the correlation of the FAS, ρ_ϵ, has a significant effect on structural fragilities. We begin with a short summary of the four main components of Pacific Earthquake Engineering Research Center's (PEER) Performance Based Earthquake Engineering (PBEE) framework, and we use this framework to define structural risk in terms of structural fragility and seismic hazard. We then describe a method for developing structural fragilities from ground motion simulations, and show that ρ_ϵ is a critical feature of ground motions that should be considered as a validation parameter for numerical simulations. A method is developed for generating simulated ground motions with appropriate ρ_ϵ. We present an example seismic risk assessment for a generic site in southern California using this ground-motion simulation method, and compare with results using the same simulation method but without the correlation. Finally, we illustrate how the effect of ρ_ϵ propagates through to the structural response variability and then into seismic risk.

2. Structural Risk in Performance Based Earthquake Engineering

Following [17], PEER's probabilistic framework for PBEE is separated into four main analysis steps: hazard analysis (characterized by a ground motion Intensity Measure, IM), structural analysis (characterized by an Engineering Demand Parameter, EDP), damage analysis (characterized by Damage Measure, DM), and loss analysis (characterized by a Decision Variable, DV). Using this framework, one can focus solely on the first two analysis steps to estimate the EDP hazard, defined as the mean annual rate of exceeding a given structural response level. The EDP hazard (also referred to as 'drift hazard') is given by Eq. 2:

$$\lambda(EDP > z) = \int_x P(EDP > z | IM = x) \, |d\lambda(IM > x)| \qquad (2)$$

where $\lambda(EDP > z)$ is the mean annual rate of exceeding EDP value z. $P(EDP > z | IM = x)$ is the structural fragility, which is the probability of exceeding EDP value of z given $IM = x$. $\lambda(IM > x)$ is the mean annual rate of exceeding IM value x, and $d\lambda$ is the rate of occurrence of IM value x, which is the slope of the IM hazard curve. Therefore, the EDP hazard for exceeding a specified value z is comprised of two quantities: the structural fragility, and the ground motion hazard, integrated over all relevant IM levels, x.

In this paper, the selected IMs are 5% damped pseudo-spectral acceleration (PSA) and Fourier amplitude spectra (FAS), and the selected EDP is the maximum interstory drift ratio (MIDR), but it is noted that the EDP risk framework (Eq. 2) is applicable to other appropriate IMs and EDPs.

Fragilities Developed from Simulations

A fragility function specifies the probability of a structural consequence (EDP) as a function of the ground motion intensity (IM). Fragility functions can be obtained by performing the Incremental Dynamic Analysis (IDA) procedure as a means of integrating structural simulations and ground motions ([17], [18]). With this procedure, using a suite of ground motions, structural response calculations are carried out in which the building is subjected to the input ground motions having a specified IM amplitude, and the fraction of the ground motions exceeding the specified EDP are counted. The process is repeated at increasing IM levels to obtain the probability of exceeding the EDP at discrete IM amplitudes. A lognormal cumulative distribution function can be fit to the logarithm of the probabilities, e.g Eq. 3:

$$P_{fit}(EDP > z | IM = x) = \Phi\left[\frac{\ln(x) - \ln(\alpha)}{\beta}\right] \tag{3}$$

where $P_{fit}(EDP > z | IM = x)$ is the fitted fragility function, Φ is the CDF of the standard normal distribution, α is the IM with median fragility, β is the logarithmic standard deviation of the CDF, and α and β are estimated from the IDA results. This method is demonstrated in Section 4. An alternative to IDA is the Multiple Stripe Analysis (MSA) method, where ground motions selected specifically for the site and IM amplitude are analyzed, instead of scaling one set of ground motions for multiple IM amplitudes [13]. The MSA method is appropriate for a site-specific risk assessment, but requires additional analysis effort. This approach is not utilized herein, because the impact of the correlation can be demonstrated using an IDA.

3. Incorporating ρ_ϵ into Ground Motion Simulations

The point source (PS) stochastic method for simulating earthquake ground motions, which is based on the pioneering work of [19], [20] and [21], among others, has been developed and refined over several decades. David Boore formalized the method and extended it to the simulation of acceleration time series ([21], [22]). With the [22] method (Boore03 hereafter), a simulated time series is produced using a seismological model of the Fourier amplitude spectrum, and assuming the spectrum is distributed with random phase angles over a time duration related to the earthquake magnitude and the distance between the source and site. The fundamentals and theory of the PS stochastic method are not covered here further because they have been described extensively in the literature. The reader is referred to [22] for a comprehensive description, as we only provide a brief summary here.

The classic procedure starts by generating normally distributed noise (Fig 2a) and applying a time domain taper with duration consistent with the scenario being considered (Fig. 2b). The tapered noise is transformed into the frequency domain (Fig. 2c), and the FAS of the noise is normalized by the square root of the mean power, such that the FAS has mean power of one (Fig. 2d, showing the natural logarithm of these values). The normalized FAS is then shaped to the PS Fourier amplitude spectrum of the considered scenario (Fig. 2e), and inverse transformed to the time domain using the phase angles from the tapered time domain noise (Fig. 2f).

The Boore03 procedure generates ϵ values from time-domain white noise, resulting in ϵ with no correlation between frequencies. To generate simulated time series with realistic inter-period

correlation, we modify the Boore03 procedure in the following ways. First, we make use of the symmetric, positive definite covariance matrix (Σ) for the inter-frequency ρ_ϵ of FAS which the authors have developed in [23]. This matrix is factorized using the Cholesky decomposition $\Sigma = LL^T$, where L is a lower triangular matrix [24]. Then the zero-mean correlated random variables Y can be calculated as Y = LZ, where Z are random variables drawn from a standard normal distribution. The random variables Y are then normally distributed with zero mean and covariance matrix Σ. In step d from Fig. 2, ϵ values are replaced with random numbers sampled in this fashion. We then multiply the sample ϵ by a standard deviation equal to 0.65 (ln units). The value of 0.65 is consistent with the Boore03 procedure FAS variance, which is not sensitive to the time-domain variance of input white noise. Finally, we proceed with the Boore03 recipe to generate time series with realistic inter-frequency ρ_ϵ of FAS.
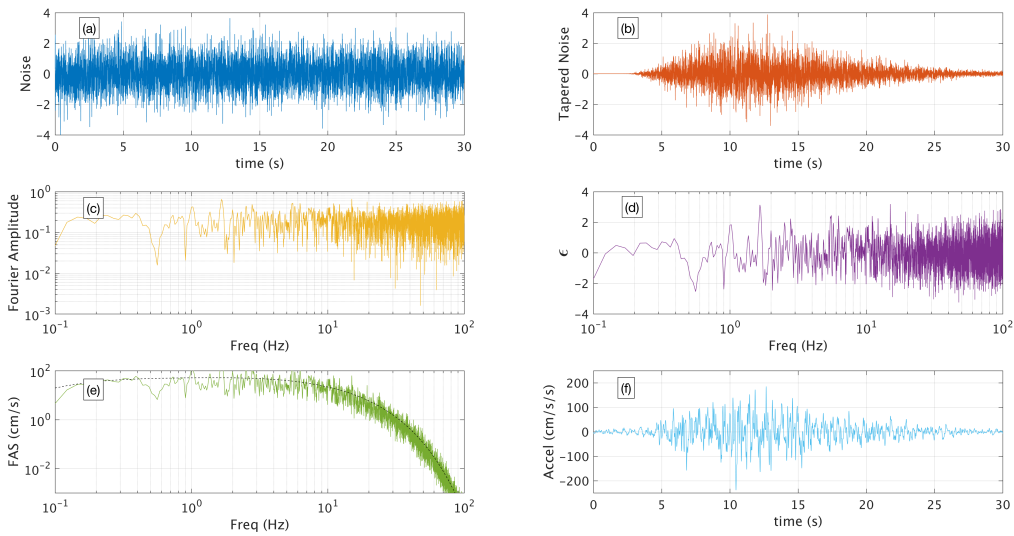

Figure 2. Illustration of the Boore (2003) procedure for simulating acceleration time series using the point-source stochastic method. Each sub-panel is described in the text.

These two simulation procedures result in a pair of compatible acceleration time series. Both have similar phasing, duration, frequency content, and amplitudes. Individual realizations of correlated ϵ may be positive or negative for frequency bands, but as the sample size is increased, the sampled ϵ have the intended standard-normal parameter values.

4. Structural Risk using Ground Motion Simulations

First, we develop structural fragilities using an IDA with two sets of ground motions, created using the two simulation procedures described previously. The first set of ground motions have near zero inter-period correlation and the second have realistic inter-period correlation. We develop suites of 500 uncorrelated and correlated ground motions using the same point source Fourier amplitude spectrum as the basis for the ground motion amplitudes. Both suites have similar ground motion distributions in FAS space (approximately 0.65 ln units), as shown in Figs 3 and 4, respectively. To obtain PSA, we perform the inverse Fourier transform to get acceleration time histories, and calculate the response spectrum. On the right side of Figs. 3 and 4, we also plot the random vibration theory (RVT) spectrum derived from seismological parameters consistent with the point

source spectrum [25]. The median PSA of the suite of 500 ground motions closely matches the RVT spectrum in both cases.

Although they have the same median, Figs. 3 and 4 illustrate the substantial differences in the distribution of PSA between the uncorrelated and correlated ground motion sets. This happens because PSA spectra are influenced by a range of frequencies. As described previously, considering broad (highly correlated) spectra, the ground motions with extreme FAS ϵ at given period generally stay extreme over the range of periods influenced by the response spectrum calculation (i.e. troughs remain in troughs, and peaks remain in peaks). The aggregate effect is the variability in PSA is higher for ground motions with realistic ρ_ϵ than for ground motions with low ρ_ϵ. The response spectrum is a simplified version of a real structure, and therefore its behavior mimics what we expect to see with the complete structural analysis.
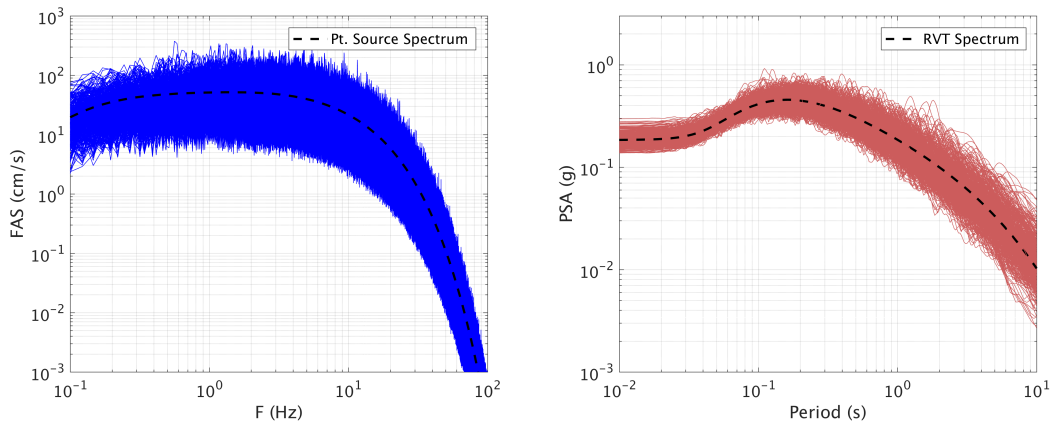

Figure 3. A suite of 500 uncorrelated ground motion simulations for a **M**7.0 scenario at 30 km. Left: FAS realizations in blue, and the point source scenario spectrum in black. Right: PSA spectra realizations in red, and the RVT spectrum in black.
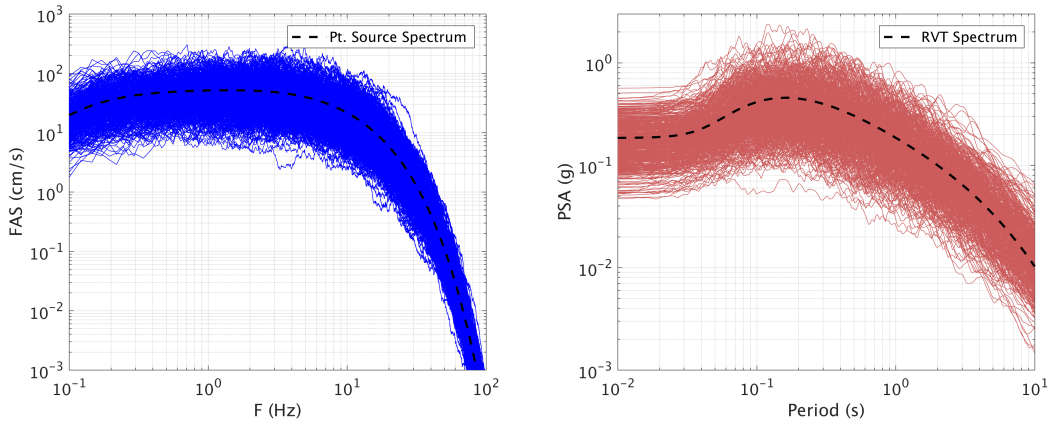

Figure 4. Like Fig. 3, but using the correlated ground motion simulations procedure.

Using the IDA approach, these sets of ground motions are scaled and numerical structural simulations are carried out. We use the open source finite-element platform, OpenSees, to perform the dynamic nonlinear structural analyses. Multiple structures have been analyzed (e.g. those described in [26], [27], and [28]). At the time of writing, our conclusions regarding the variability in structural response do not vary with structure type. Since the impact of the correlation is related

to structural softening, we intend to explore the effect on additional structures, including those with short fundamental periods, to confirm that our observations are applicable to a wide range of structures. The fragility results presented herein are for the 6-story steel special moment-resisting frame (SMRF) building model described in [26].

The IDA results are presented in Fig. 5, where blue symbols and lines represent data from the uncorrelated simulations and the red symbols and lines represent the correlated simulations. For each PSA level (at the fundamental structural period; T=1.38 s), the fraction of the ground motions exceeding 4% MIDR are counted. The process is repeated over multiple IM levels to obtain the probability of exceeding 4% MIDR at the discrete IM amplitudes. The natural logarithms of these probabilities are fit to a lognormal CDF as described in Section 2. For the presented results, the lognormal CDF dispersion parameter, β, is 0.31 for the uncorrelated ground motions and 0.52 for the correlated ground motions (comparable to the building code value 0.6 [29]). Larger β values mean flatter fragility curves with higher probabilities at the low IM levels.
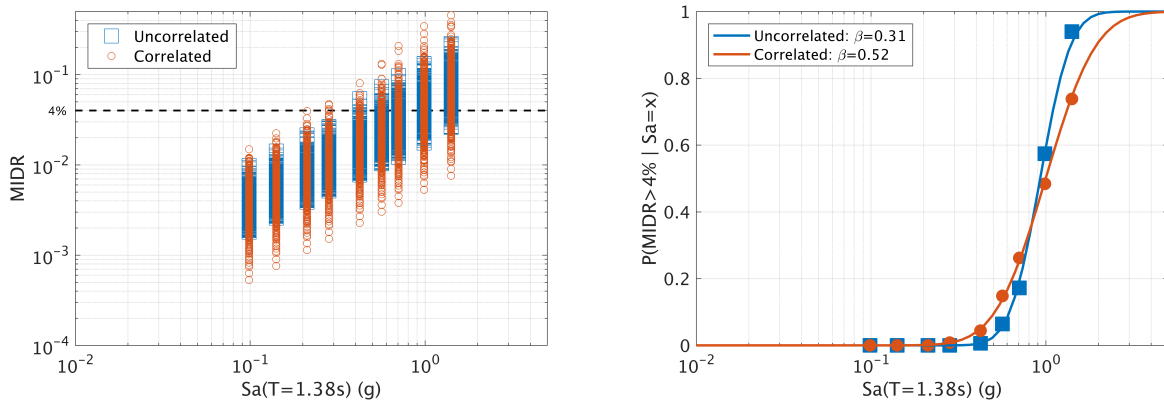

Figure 5. Left: MIDR results of the structural analysis for suites of 500 ground motions at. Right: MIDR>4% probabilities (symbols) and the fitted CDF fragility functions (lines).
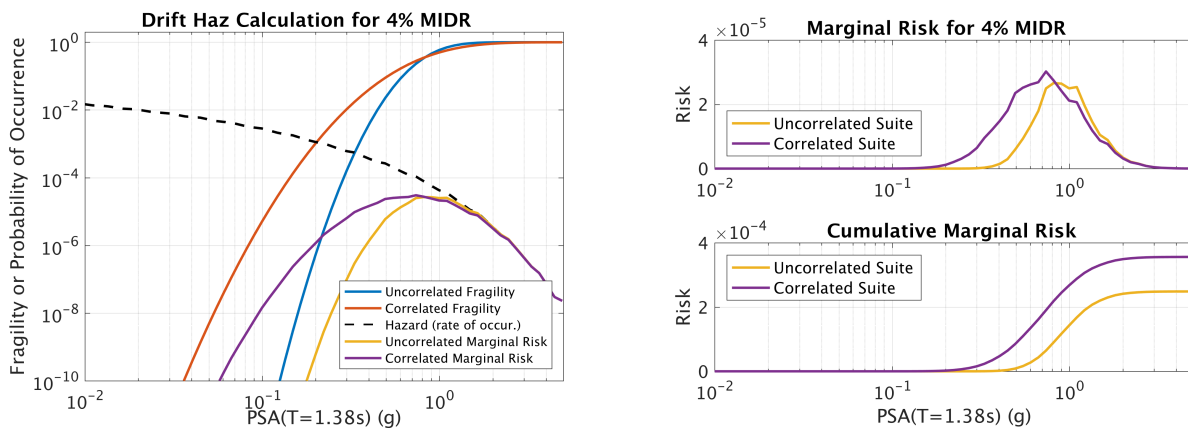

Figure 6. Left: Combining the seismic hazard occurrence and MIDR>4% fragilities to get the EDP hazard. Right: the marginal risk and cumulative marginal risk on linear scales.

We combine the structural fragilities with the seismic hazard to calculate the EDP hazard, using Eq. 2. The results are shown in Fig. 6, where the left panel compares the structural fragilities and

marginal risk on a logarithmic vertical axis. Plotting them this way illustrates the consequential differences between them at moderate IM levels, where the hazard is higher, and the risk is sensitive to the fragility. To calculate the risk from the EDP hazard, we have assumed a step function of the DMs (usually collapse) as a function of EDP fragility. The right panels of Fig. 6 compare the marginal and cumulative marginal risk on a linear scale for the two ground motion sets. For this case, the highest marginal risk comes from PSA(T=1.38 s) levels less than 1g. We have looked at structural risk for four damage states using MIDR exceedances of 0.5%, 1%, 2%, and 4% (Table 1). For the MIDR>4% case, the structural risk calculated using the ground motions with realistic inter-period correlations is a factor of 1.43 higher than the risk calculated using uncorrelated ground motions, which corresponds to approximately the difference between a 4,000- and 2,800-year return period.

Table 1.   Structural risk for damage states with MIDR exceedances of 0.5%, 1%, 2%, and 4%.

GM Suite	MIDR ≥ 0.5%	MIDR ≥ 1%	MIDR ≥ 2%	MIDR ≥ 4%
Correlated	1.44E-02	5.12E-03	1.42E-03	3.56E-04
Uncorrelated	1.25E-02	4.26E-03	1.11E-03	2.49E-04
Ratio	1.15	1.20	1.28	1.43

5. Conclusions

This paper demonstrates that the inter-period correlation of epsilon (ρ_ϵ) is an essential component of ground motion simulation validation, particularly when the simulations are used in structural fragility or risk applications. Without the adequate inter-period correlation of simulated ground motions, variability in the structural response may be under-estimated. This leads to structural fragilities which are too steep (under-estimated dispersion parameter β) and propagates through to non-conservative estimates of seismic risk. The conclusions herein apply directly to structural fragility or risk assessments which are derived from ground motion simulations, commonly referred to as 'ruptures to rafters' simulations.

6. References

1. Al Atik L, Abrahamson NA, Cotton F, Scherbaum F, Bommer JJ, Kuehn N. The variability of ground-motion prediction models and its components. *Seismological Research Letters,* 2010; **81(5)**:794-801.

2. Fisher RA. *Statistical Methods for Research Workers*, 13th Ed., Hafner, 1958.

3. Abrahamson NA, Silva WJ, Kamai R. Summary of the ASK14 Ground Motion Relation for Active Crustal Regions. *Earthquake Spectra*, 2014*;* **30**:1025-1055. doi: 10.1193/070913EQS198M

4. Al Atik L. Correlation of spectral acceleration values for subduction and crustal models. In: COSMOS Technical Session, Emeryville, CA, 2011.

5. Akkar S, Sandıkkaya MA, Ay BÖ. Compatible ground-motion prediction equations for damping scaling factors and vertical-to-horizontal spectral amplitude ratios for the broader Europe region. *Bull Earthq Eng* 2014; **12**:517–547. doi: 10.1007/s10518-013-9537-1

6. Azarbakht A, Mousavi M, Nourizadeh M, Shahri M. Dependence of correlations between spectral accelerations at multiple periods on magnitude and distance. *Earthq Eng Struct Dyn* 2014; **43**:1193–1204.

7.   Jayaram N, Baker JW, Okano H, Ishida H, McCann MW, Mihara Y. Correlation of response spectral values in Japanese ground motions. *Earthquakes and Structures*; 2011; **2(4):**357–376.

8.   Baker JW, and Cornell CA. Correlation of Response Spectral Values for Multi-Component Ground Motions, *Bulletin of the Seismological Society of America*, 2006; **96 (1),** 215-227.

9.   Baker JW, and Bradley BA. Intensity measure correlations observed in the NGA-West2 database, and dependence of correlations on rupture and site parameters. *Earthquake Spectra,* 2017 (in press).

10. Baker JW, and Jayaram N. Correlation of spectral acceleration values from NGA ground motion models. *Earthq Spectra* 2008; **24**:299–317. doi: 10.1193/1.2857544

11. Cimellaro GP. Correlation in spectral accelerations for earthquakes in Europe. *Earthq Eng Struct Dyn* 2013; **42**:623–633. doi: 10.1002/eqe.2248

12. Goda K, Atkinson GM. Probabilistic Characterization of Spatially Correlated Response Spectra for Earthquakes in Japan. *Bull Seismol Soc Am* 2009; **99:**3003–3020. doi: 10.1785/0120090007

13. Stafford PJ. Inter-frequency correlations among Fourier spectral ordinates and implications for stochastic ground-motion simulation, *Bulletin of the Seismological Society of America,* 2017 ISSN: 1943-3573

14. Bayless J, and Abrahamson NA. An empirical model for Fourier amplitude spectra using the NGA-West2 database, in preparation, 2017.

15. Lin L, Naumoski N, Foo S, and Saatcioglu M. Elongation of the fundamental periods of reinforced concrete frame buildings during nonlinear seismic response, presented at the 14th World Conf Eqk Eng, Beijing. 2008

16. Bradford SC. *Time-frequency analysis of systems with changing dynamic properties.* Dissertation (Ph.D.), California Institute of Technology. 2007.

17. Moehle JP, and Deierlein GG. A framework methodology for performance-based earthquake engineering. Paper presented at the 13th World Conference on Earthquake Engineering, Vancouver. 2004

18. Baker, JW. Trade-offs in ground motion selection techniques for collapse assessment of structures. Vienna Congress on Recent Advances in Earthquake Engineering and Structural Dynamics. Vienna, Austria. 2013.

19. Brune JN. Tectonic stress and spectra of seismic shear waves from earthquakes, *J. Geophys. Res*. 1970; **75**, 4997–5009.

20. Hanks TC, and McGuire RK. The character of high-frequency strong ground motion, *Bull. Seismol. Soc. Am*. 1981; **71**, 2071–2095.

21. Boore DM. Stochastic simulation of high-frequency ground motions based on seismological models of the radiated spectra, *Bull. Seismol. Soc. Am*. 1983; **73**, 1865–1894.

22. Boore DM. Simulation of ground motion using the stochastic method, *P&A Geophysics.* 2003; **160**, 635-675.

23. Bayless J, and Abrahamson NA. An empirical model for the inter-period correlation of FAS ϵ, in prep. 2017.

24. Seydel RU. *Tools for Computational Finance*, Universitext, Springer-Verlag London Limited 2012

25. Boore DM and Thompson EM. Empirical improvements for estimating earthquake response spectra with random-vibration theory, *Bull. Seismol. Soc. Am*. 2012; **102(2)**, 761-772

26. Kalkan E and Kunnath SK. Effects of Fling Step and Forward Directivity on Seismic Response of Buildings. *Earthquake Spectra*, 2006; **22**, No. 2, 367–390.

27. Heo YA. *Framework for Damage-Bassed Probabilistic Seismic Performance Evaluation of Reinforced Concrete Frames*. Dissertation (Ph.D.), UC Davis. 2009.

28. Kunnath SK, Erduran E, Chai YH, and Yashinsky M. Effect of Near-Fault Vertical Ground Motions on Seismic response of Highway Overcrossings. *J. Bridge Engineering*, 2008; **13(3)**, 282-290.

29. ASCE. 2016. Minimum Design Loads for Buildings and Other Structures. ASCE/SEI Standard 7-16.